DIPARTIMENTO DI FISICA "GALILEO GALILEI"
UNIVERSITA' DEGLI STUDI DI PADOVA

I.N.F.N-ISTITUTO NAZIONALE DI FISICA NUCLEARE
SEZIONE DI PADOVA

DFPD/ 37/ 85

STUDY OF A LEAD GLASS-CALORIMETER WITH VACUUM PHOTOTRIODE READ-OUT

P. CHECCHIA, G.GALEAZZI, U.GASPARINI, M.MAZZUCATO,
M. PEGORARO, L.VENTURA, G.ZUMERLE.
DIPARTIMENTO DI FISICA - UNIVERSITA' E SEZIONE INFN, PADOVA, ITALY

A. LOPEZ
DEPARTAMENTO DE FISICA FUNDAMENTAL, UNIVERSIDAD SANTANDER, SPAIN

F. BIANCHI, E.MENICHETTI, A.ROMERO, S.RUSTICHELLI.
DIPARTIMENTO DI FISICA - UNIVERSITA' E SEZIONE INFN, TORINO, ITALY.

E. CASTELLI, L.LANCERI, P. POROPAT.
DIPARTIMENTO DI FISICA - UNIVERSITA' E SEZIONE INFN, TRIESTE, ITALY.

A. FERRER, J.J.GOMEZ, J.VELASCO.
IFIC, CENTRO MIXTO UNIVERSIDAD, CSIC BURJASOT, VALENCIA, SPAIN.

STUDY OF A LEAD-GLASS CALORIMETER WITH VACUUM PHOTOTRIODE READ-OUT

P. Checchia, G. Galeazzi, U. Gasparini, M. Mazzucato, M. Pegoraro,
L. Ventura, G. Zumerle.
Dipartimento di Fisica dell'Università e Sezione INFN, Padova, Italy

A. Lopez.
Departamento de Fisica Fundamental, Universidad, Santander, Spain

F. Bianchi, E. Menichetti, A. Romero, S. Rustichelli.
Dipartimento di Fisica dell'Università e Sezione INFN, Torino, Italy

E. Castelli, L. Lanceri, P. Poropat.
Dipartimento di Fisica dell'Università e Sezione INFN, Trieste, Italy

A. Ferrer, J.J. Gomez, J. Velasco.
IFIC, Centro Mixto Universidad, CSIC Burjasot, Valencia, Spain

ABSTRACT

A prototype calorimeter of lead glass bars read by one-stage vacuum photomultipliers (triodes) has been tested at CERN with electrons in the energy range 2-30 GeV. Different glass-triode combinations have been compared. An electronic amplification noise corresponding to about 30 MeV has been obtained. The space resolution has been measured to be 4.4 mm on average.

1. INTRODUCTION

The end-cap electromagnetic calorimeters of the DELPHI experiment at LEP will be built using a fine grained matrix of lead glass counters pointing to the interaction region. They will consists of approximately 100 modules of about 100 counters each.[1]

Being located in a region of high magnetic field, 1.2 T, the glass will be instrumented with newly developed one-stage photomultipliers ("triodes").[2]

With this arrangement, keeping the good energy and position resolution typical of conventional lead glass calorimeters equipped with photomultiplier tubes [3,4] is not a trivial task, especially at energies in the GeV range. The relatively low light output, typically 1000 photoelectrons/GeV, and the low gain of the phototriodes, of the order of 10 in the first prototypes, require an electronic amplification of very high gain. Since there is an intrinsic lower limit on the noise of the electronic amplification stage, of about 200 e^- r.m.s. in our conditions, every detector component has to be optimized to give the best possible output, if we want to keep the the counter noise in the 20 MeV range.

Two lead glass producers, Corning France and Schott, and three photomultiplier makers, EMI, Hamamatsu and R.T.C., have accepted to collaborate in this optimization effort.

The following parameters have been studied:

a) internal transmission of the glass,

b) surface matching between photocathode and glass,

c) quantum efficiency for Cherenkov light,

d) triode gain with and without magnetic field,

e) electronic noise induced by the triode structure.

After successful tests on single counters we have built a full scale prototype module of about 100 counters that was exposed to a test beam at CERN in summer 1984.

The aims were:

- to measure precisely the light output of different glass types,
- to compare the results of triodes of different makers,
- to determine the energy and position resolution,
- to measure the noise expressed in terms of energy (GeV) in a situation as close as possible to the final experimental set-up. This parameter determines in fact the performance of such a kind of detector.

In this paper after a brief description of the DELPHI Forward Electromagnetic Calorimeter (FEMC) we report on the results obtained with such a prototype module.

2. The DELPHI F.E.M.C.

2a) Geometry

The e.m. calorimeter on each of the two end-caps is a disc of 480 cm diameter, placed at 284 cm from the interaction point, covering the theta region from 8° to 35.5°.

We have chosen an angular granularity of about 1°, that gives a cross section for the counters of the order of 5x5 cm. This also corresponds to the lateral size of e.m. showers, thus allowing a good space

resolution through center of gravity methods[3].

We have in addition adopted a quasi-pointing geometry for several reasons:

a) the overlap of showers from different particles is minimized,

b) the energy of a shower is spread over a small number of counters, thus improving the energy resolution at low energies,

c) the small aberration (about 3°) from perfect pointing minimizes the negative effects of the dead spaces introduced by the supporting structures.

To achieve this geometry, the glass absorbers have the shape of a truncated square pyramid, of front face 50x50 mm^2 and opening angle 13.6 mrad, except three rows (columns) on either side of the horizontal (vertical) diameter, where the blocks have two parallel and two diverging lateral faces.

2b) Mechanical Support

A typical module (see Fig. 1) contains 96 counters, arranged in 12 columns of 8 counters each. It is built with non-magnetic steel plates. The top and bottom plates are 3 mm thick, while the lateral walls are 1 mm thick.

The box is internally reinforced by vertical plates, 1 mm thick, placed between every second column of counters. These plates are also used to fix the blocks in position.

The non-active surface of the module is about 2% of the total surface. The modules are supported from the back with rails that allow their extraction without disturbing the detectors in front.

The mechanical deformations of the module under full load have been measured to be smaller than 1 mm.

The longitudinal thickness of the absorbers has been fixed to be at least 20 X_0. Given the available space, the glass radiation length must be not greater than 22 mm.

3. THE PROTOTYPE MODULE

The module shown in Fig. 1 has been built for prototype tests.

The different glass-triode combinations placed in the module are given in Table I.

TABLE I

Triode / Glass	HAMAMATSU R 2184	RTC XP 1201	EMI D 435
CORNING CEREN 22 (Xo=22 mm)	23	8	==
SCHOTT SF1 (Xo=22 mm)	16	==	2
SCHOTT SF6 (Xo=17 mm)	6	2	==

The electronic amplification chain was the same for all the counters, and all connections and cable lengths were very close to the final ones.

The longitudinal dimension of the triode prototypes including the housing for the high voltage divider and the preamplifier is 58 mm, 87 mm, 75 mm for Hamamatsu, RTC and EMI types respectively.

The glass blocks were laterally wrapped with aluminized mylar and black tape. Fig. 2 is a picture of a completely assembled counter, together with two triodes of different type and a preamplifier in its housing.

The triode is optically coupled to the glass with silicon grease[5]. The glass face opposite to the triode is left open, to allow the coupling to the optical monitoring system. Wrapping this face would increase the output signal by 10%.

The low noise hybrid preamplifier is mounted close to the base of the triode, to minimise the connecting lead capacitance.

The triodes have been operated at the relatively low voltage of 700 V. The cathode-dynode and dynode-anode voltages were kept in a ratio 1:1, using a resistive voltage divider of 20 M Ω, see Fig. 3.

At this voltage the average value and the dispersion (r.m.s.) of the gain for the three triode types, measured by the manufacturers, are:

HAMAMATSU R2184	9.5 ± 0.9
RTC XP1201	13.5 ± 2.9
EMI D435	8.4 --

We stress once again that the triodes used are prototypes. The quality in the final production is likely to be improved.

4. ELECTRONIC CHAIN

The amplification chain is described in detail in Ref. 6. We will review here the main characteristics.

To minimize the power dissipation inside the detector, only the first amplification stage has been put on the back of the triode. The signal is then sent through 50 m of twisted pair cable to a further amplification and shaping stage. The peak value of the output signal is digitized with a 12-bit LeCroy 2280 charge ADC, using a gate width of 150 ns. Data were read by CAMAC using a VAX 750 computer and written onto magnetic tape for off-line analysis.

The preamplifier is based on a commercial hybrid from LABEN, type 5254, with FET input stage, suitably modified to make full use of the very low capacitance of our detector and of the low counting rates typical of the LEP collider.

The amplification and shaping module has been specially developed in our labs for this application (Fig. 4). The design has been kept very simple, bearing in mind the large number of channels to equip.

The first stage consists in a differential receiver that performs a first integration with a time constant of 0.5 µs. It is followed, after a pole-zero cancellation, by a second approximate integration that completes the shaping and by a driver for coaxial cable. In spite of its

limited number of components such a device exhibits anyway a signal to noise ratio that differs by no more than 25% from the optimum theoretical limit.

Fig. 5 shows typical ENC (Equivalent Noise Charge) values of one of the hundred electronic channels, mounted for the test, as a function of the input capacitance. The shaping time is 2 µs. The mean, over the whole sample, of the open circuit input noise level is $\langle ENC \rangle = 145\ e^-$ r.m.s.

When coupled to the triodes, as shown in Fig. 3, the input shunt capacitance and additional noise sources, such as the protection diode, the triode dark current, the voltage divider resistors and the AC coupling bring the noise to the level of $220\ e^-$ r.m.s.

This figure is considerably increased, when the HV is applied in the presence of acoustic vibrations, that cause an oscillation in the effective detector capacitance.

For the data of the test, this effect could be only partially corrected off-line using the correlation between different channels of this particular noise source. The final noise level for these data remains however 30% higher than the laboratory results.

In a subsequent version of the shapers, tested in the same beam environment a few months later, this effect has been completely cured mainly by the adoption of a bipolar shaping that acts as an additional low frequency filter. The resulting noise level, with this new chain is about $250\ e^-$ r.m. s. and does not generally show any dependence on the value of the HV applied.

The deviation from linearity of this system has been measured to be less than 0.5% at full scale which corresponds to an energy release of

50 GeV.

The amplification uniformity between different channels is better than 5%.

5. EXPERIMENTAL PROCEDURE

The prototype has been tested in the X7 beam at the CERN SPS.

The electrons were selected with the help of a threshold Cherenkov counter. The beam coordinates were defined by two 4 mm pitch MWPC, with 5 planes each situated at a distance of 10 and 24 metres from the module.

The module was placed on a movable platform[7], with four independent movements, so that it was possible to choose for each counter, not only its position, but also the angle of its axis with respect to the beam.

The beam energy could be varied from 2 to 30 GeV with a spread $\sigma_E/E = 0.5\ \%$

The beam intensity was up to 2000 particles in a spill time of 2.2 seconds.

Each counter was centered to the beam, with its axis aligned to the beam direction, and a sample of about 2000 shower data collected to calibrate the energy response of the detector.

For the SF6 glass we could also perform an energy scan from 2 to 30 GeV/c, with good beam conditions.

Since the study of the spatial precision requires a low energy beam of good quality, a separate special run has been done at the CERN PS, using a small matrix of seven blocks of SF1 glass. In this run, the beam size was defined by a small scintillation counter (10x3 mm^2) situated just in front of the lead glass blocks.

6. ELECTRON BEAM RESULTS

Linearity

We could not measure any deviation from linearity over the available energy range: 2-30 GeV.

Photoelectron yield and response uniformity

The calibration constants and the precise knowledge of the electronic amplification and of the triode gain (individually measured by the manufacturers) allow a determination of the photoelectron yield per unit of released energy, for each counter. It depends clearly on the glass type and only weakly on the triode type.

The average values are:

SCHOTT	SF1	642 phe/GeV
CORNING	C22	580 phe/GeV
SCHOTT	SF6	422 phe/GeV

An important feature that characterizes this new type of instrumentation is the uniformity of the overall detector response.

For the products which at the moment of the test were the most developed industrially, the SF1 glass and the Hamamatsu triode, the spread of the calibration coefficients around the average value is 11% rms, when the same high voltage is applied to all the triodes (Fig. 6). This figure is not expected to increase significantly when the triodes are operated in an uniform magnetic field. The uniformity, according to the manufacturers, is expected to improve with mass production of the components. An important consequence of this fact is a drastic simplification in the HV distribution system, since there is no need for a gain adjustment for each individual counter.

Energy resolution

We expect some degradation of the energy resolution at low energies, compared to the conventional PM results due to the electronic noise.

This extra term, when expressed in energy units, depends on the photoelectron yield and the triode amplification. For the data of the test the mean values of this noise for the different glass-triode combinations, expressed in MeV, are:

TABLE II

	HAMAMATSU	RTC	EMI
SF1	46	27	39
C22	51	30	==
SF6	77	40	==

The EMI results, being based on two triodes only, are less significant than the others.

The RTC-SF1 combination has not been measured directly but extrapolated from the other results.

The expression for the energy resolution which includes the extra term due to the electronic chain is:

$$\frac{\sigma_E}{E} = \sqrt{\left(a + \frac{b}{\sqrt{E}} \right)^2 + \left(\frac{c_n}{E} \right)^2}$$

The constants a and b are as usual due to the shower development fluctuations, c_n is the energy equivalent of the amplification noise of the combination of the n counters whose signals are summed to obtain the total energy of the shower. If the n counters are of the same type, and the correlation of the noise between different channels is negligible, C_n can be factorized as $C_n = C_1\sqrt{n}$, where C_1 is the noise of a single counter.

We can compare equation 1 with the experimental data shown in Fig. 7. Unfortunately we have to compare different glass types in the SPS and PS energy intervals, because the SPS data on SF1 glass suffered from the presence of detectors upstream of our set up, degrading the effective electron beam momentum resolution. The constant C_n for the group of 9 counters in the SPS run was 200 MeV, while for the group of 7 blocks in the PS data it was 160 MeV, according to the sum in quadrature of the noise of the individual channels.

The best fit, using the values of C_n given above, is obtained with $a=(0.4\pm0.1)$, $b=(6.9\pm0.2)\ \mathrm{GeV}^{1/2}$.

The energy spectrum measured at 2 and 20 GeV nominal beam energy is shown in Fig. 8a) and b).

7. SPACE PRECISION

With center of gravity methods, the space precision attainable in the measurement of e.m. showers depends[3] on the ratio Δ/b, where Δ is one half of the granularity of the detector (25 mm in our case) and b is the exponential lateral fall-off slope of the shower.

If Δ is not small with respect to b, the center of gravity of the signals gives a biased measurement of the shower centroid. However, algorithms exist which allow one to correct for this.

Fig. 9a) and 9b) show the quantity $F = 2\min(A_i, A_{i+1})/(A_i + A_{i+1})$

where A_i is the signal of counter i, as a function of the distance from the boundary between two adjacent counters, for electrons of 5 GeV, with angles of incidence 0° and 4° respectively, with respect to the counter axis.

Fig. 9a is symmetric, as it should be, and the slope is $b\approx5.8$ mm. Fig. 9b) has different slopes on the two sides, respectively $b_1\approx8.0$ mm and $b_2\approx5.2$ mm.

The precision attainable is equivalent in the two cases, being 4.4 mm with the beam uniformly spread across the counter.

Fig. 10a) and b) show the reconstructed average position, as a function of the impact point, and the spread around the average, for the two angles of incidence. The precision varies from 2.7 mm near the counter separation to about 6 mm for electrons hitting the center of a counter.

8. RATE LIMITS

The CR filter introduced in the last stage of our shaping amplifier generates a shift of the base line which increases linearly with the energy deposited per second on each counter. We have measured this effect, which can worsen the detector energy resolution, sampling the base line of a counter exposed to a 30 GeV electron beam. Varying the beam intensity, we have determined the base line shift as a function of the energy flux. The result shown in Fig. 11 indicates a shift of 1 count, equivalent to about 10 MeV, for an energy flux of 10^4 GeV/s.

The main energy flux in our detector in DELPHI comes from the "off-momentum" electrons generated by beam bremstrahlung in the residual gas. The mean energy deposited in the counters closest to the beam pipe has been estimated with a Monte Carlo simulation to be about 10^2 GeV/s.

9. CONCLUSIONS

We have tested a lead glass calorimeter with vacuum phototriode readout using an electron beam of 2-30 GeV.

The measured energy resolution is described by the expression:

$$\frac{\sigma_E}{E} = \sqrt{\left(0.4 + \frac{6.9}{\sqrt{E}}\right)^2 + \left(\frac{C\sqrt{N}}{E}\right)^2}$$

The constant c depends on the glass-triode combination. It can be as low as 20 MeV with the latest version of the amplification chain.

The average space resolution has been measured to be 4.4 mm for electrons of 5 GeV.

REFERENCES

1. DELPHI Progress Report, CERN/LEPC 84/16
2. M.D. Rousseau et al., IEEE Trans. Nucl. Sci., Vol NS30, 479, Feb. 83.
3. G.A. Akopdjanov et al., Nuclear Instruments & Methods 140 (77) 441.
4. B. Powell et al., N.I. &M. 198 (1982) 217.
5. Rhône-Poulenc B 431 grease.
   In the final set up the triode will be glued to the glass through an optical epoxy resin of refractive index n=1.54.
6. G. Barichello et al."Low noise amplification chain of the DELPHI end-cap e.m. calorimeter". Padova Preprint.
7. P.L. Barberis et al., DELPHI internal note 84-67/CAL-7.

FIGURE CAPTIONS

Fig. 1	The prototype module.
Fig. 2	A completely assembled counter, plus two triodes of different type and the preamplifier in its housing.
Fig. 3	The triode electrical connections and preamplifier diagram.
Fig. 4	Shaper electrical diagram.
Fig. 5	Variation of the E.N.C. with the input capacitance for a typical preamplifier.
Fig. 6	Distribution of calibration coefficients for blocks of SF1 glass read by R2184 triodes.
Fig. 7	Energy resolution.
Fig. 8	Energy distribution: a)2 GeV, b) 20 GeV nominal beam energy.
Fig. 9	Shower lateral development: a) angle of incidence 0°, b) angle of incidence 4°. $F=2\min(A_i,A_{i+1})/(A_i+A_{i+1})$.
Fig.10	Space precision: a) angle of incidence 0°, b) angle of incidence 4°.
Fig.11	Base line shift as a function of beam flux.

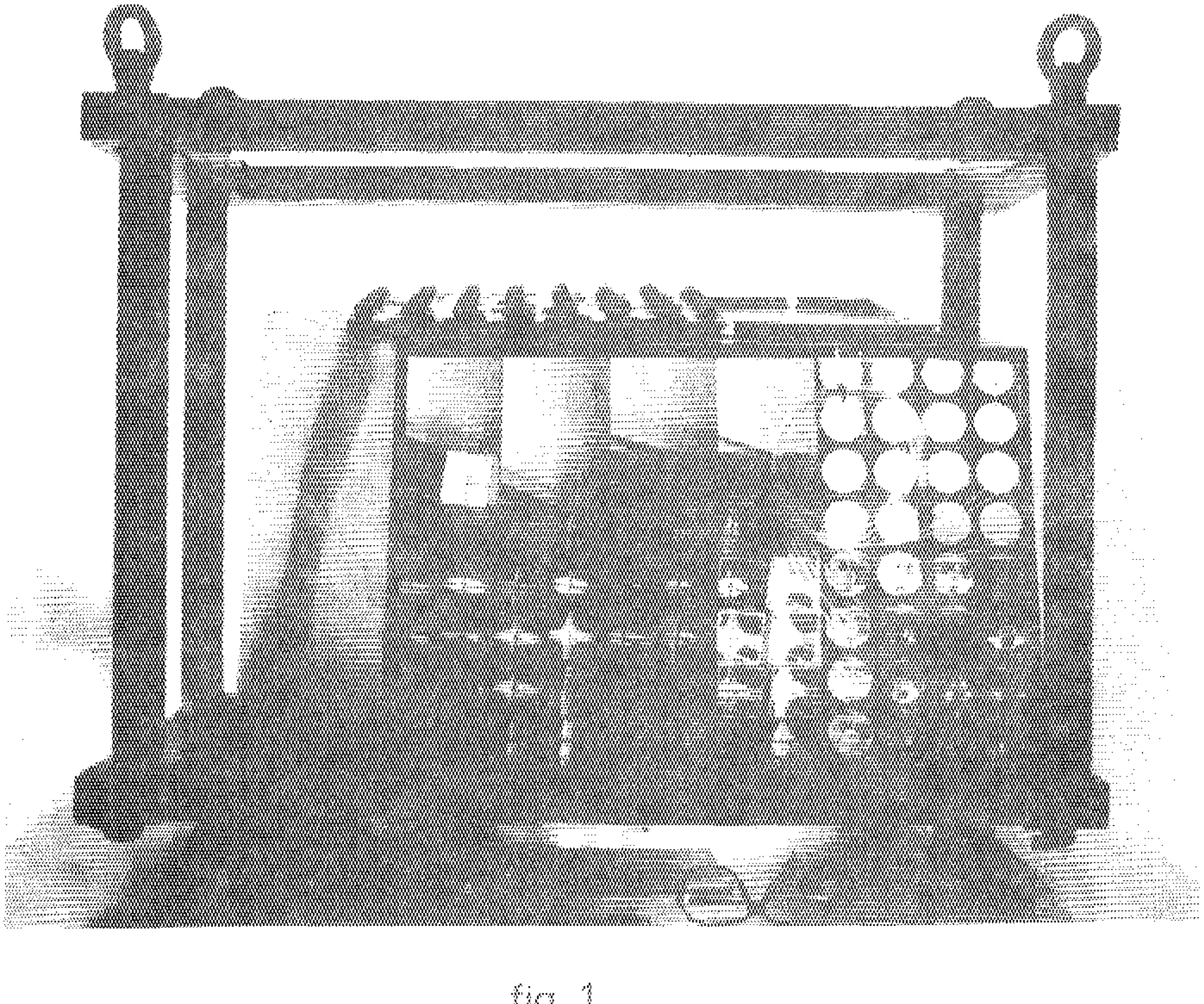

fig. 1

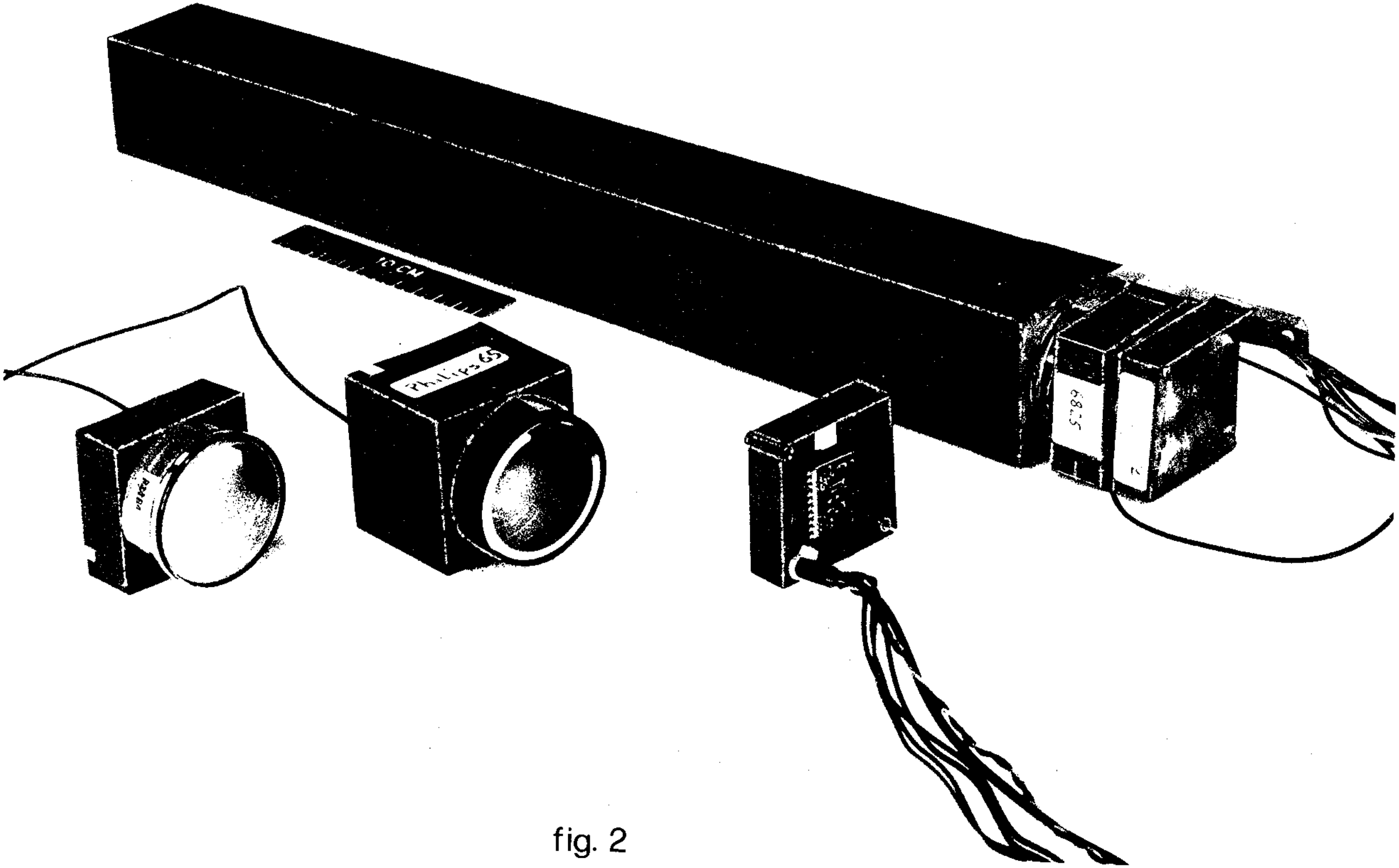

fig. 2

PREAMPLIFIER ELECTRICAL DIAGRAM

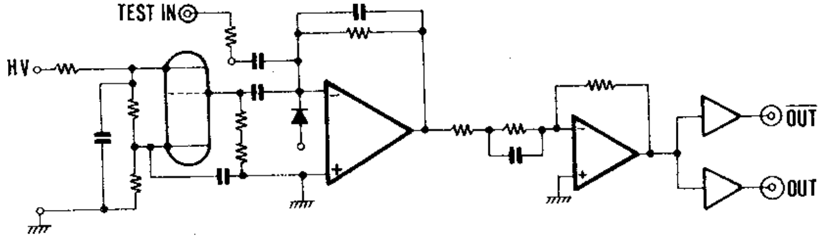

fig. 3

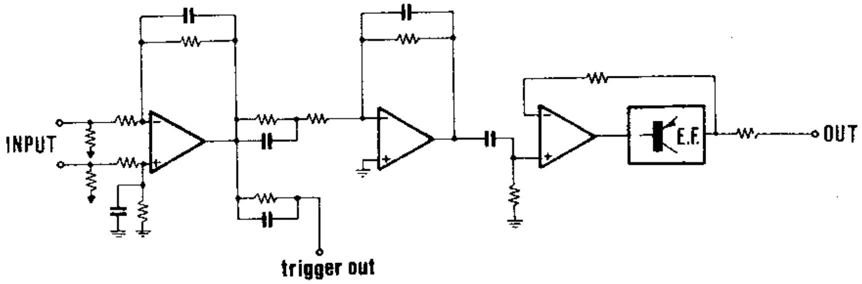

fig. 4

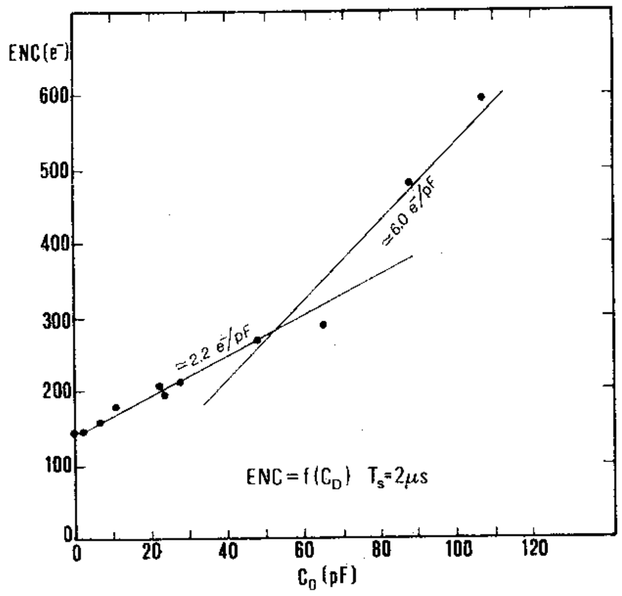
ENC(e⁻)
600
500
400
300
200
100
0
0
20
40
60
80
100
120
C_D (pF)
≃2.2 e⁻/pF
≃6.0 e⁻/pF
ENC = f(C_D) T_s = 2μs

fig. 5

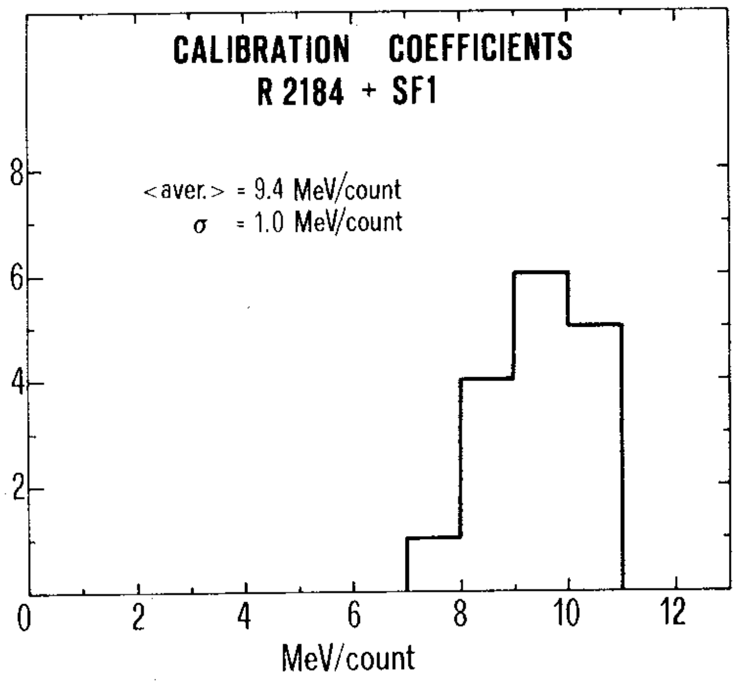
CALIBRATION COEFFICIENTS
R 2184 + SF1
<aver.> = 9.4 MeV/count
σ = 1.0 MeV/count
8
6
4
2
0
2
4
6
8
10
12
MeV/count

fig. 6

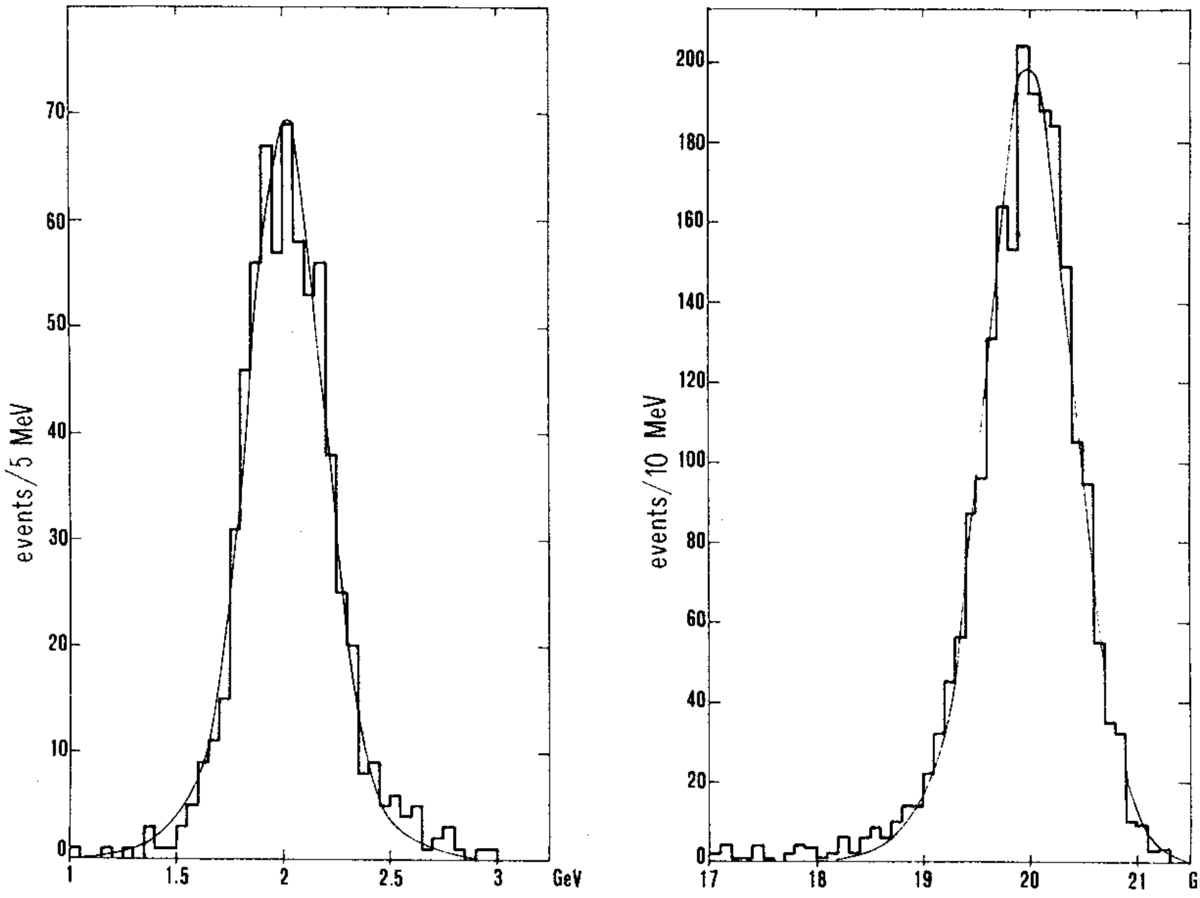
events/5 MeV
0
10
20
30
40
50
60
70
1
1.5
2
2.5
3
GeV
events/10 MeV
0
20
40
60
80
100
120
140
160
180
200
17
18
19
20
21
GeV

fig. 7

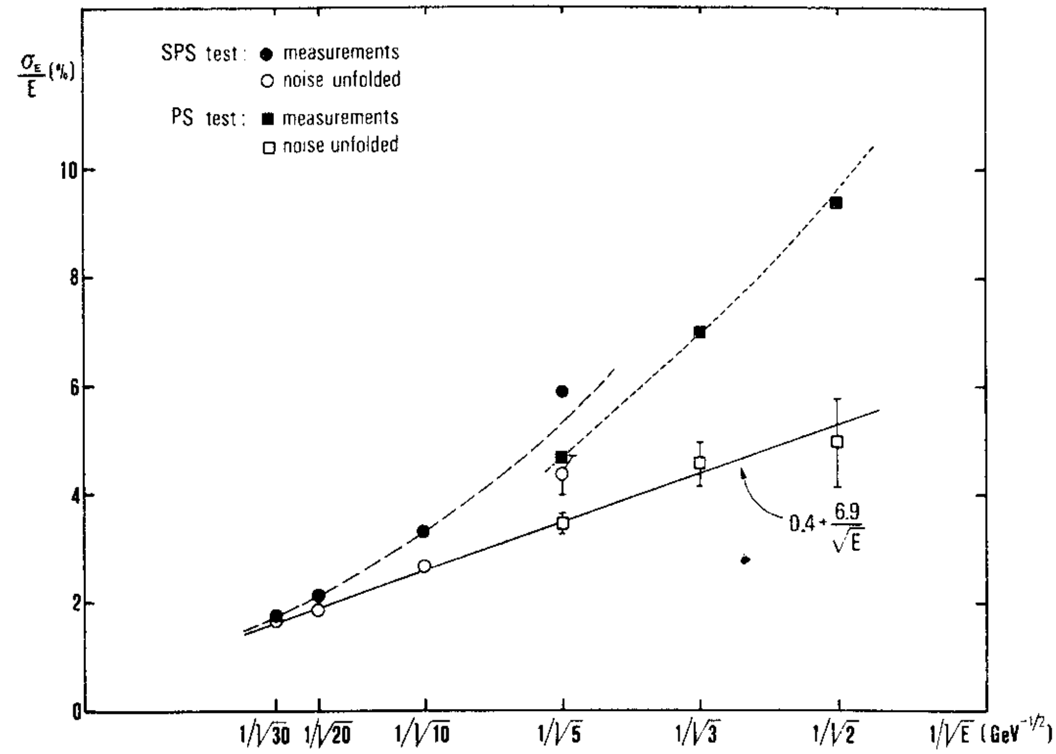
$\frac{\sigma_E}{E}$ (%)
SPS test : ● measurements
○ noise unfolded
PS test : ■ measurements
□ noise unfolded
10
8
6
4
2
0
$0.4 + \frac{6.9}{\sqrt{E}}$
$1/\sqrt{30}$
$1/\sqrt{20}$
$1/\sqrt{10}$
$1/\sqrt{5}$
$1/\sqrt{3}$
$1/\sqrt{2}$
$1/\sqrt{E}$ (GeV$^{-1/2}$)

fig. 8

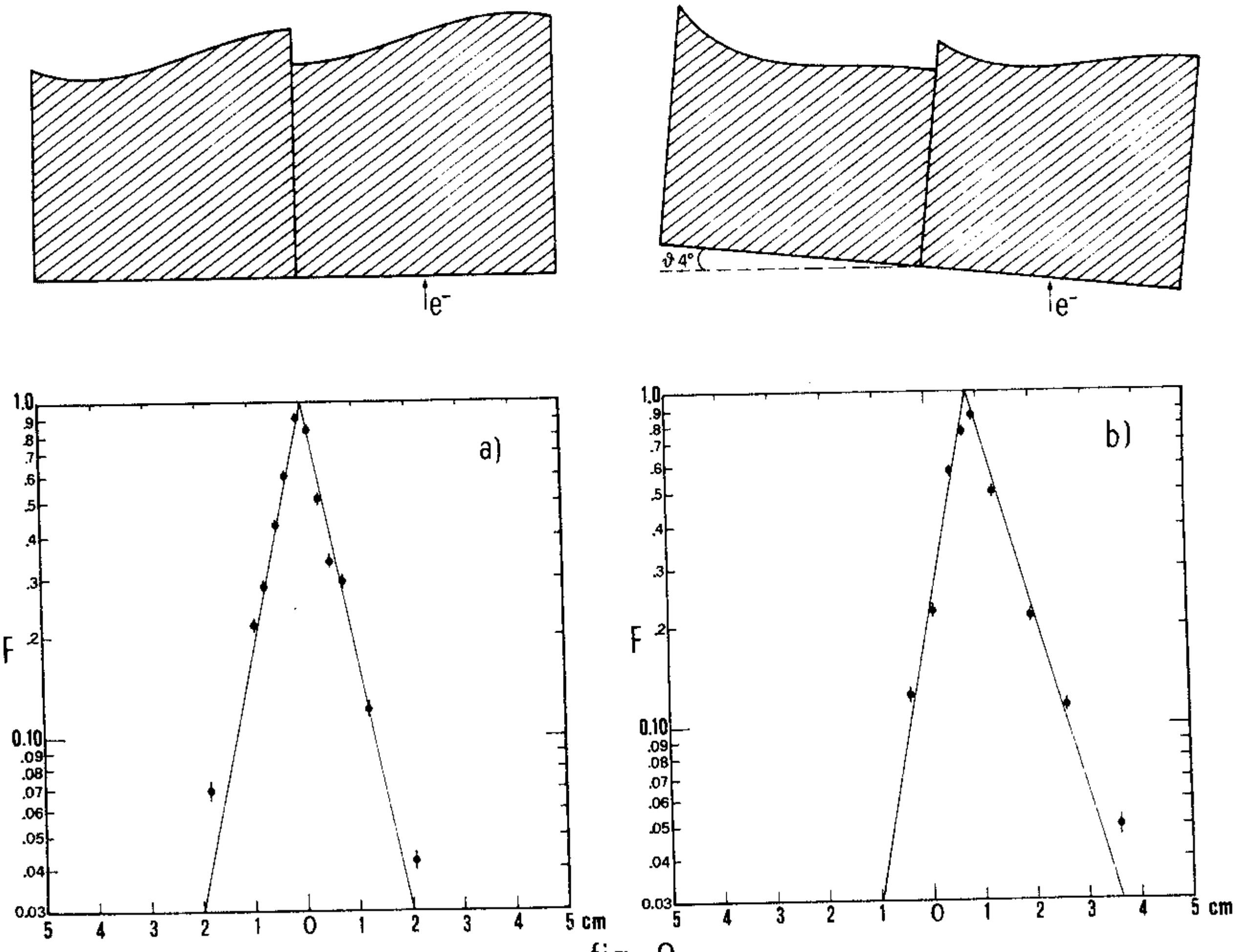
e⁻
ϑ 4°
e⁻
a)
b)
F
1.0
.9
.8
.7
.6
.5
.4
.3
.2
0.10
.09
.08
.07
.06
.05
.04
0.03
5
4
3
2
1
0
1
2
3
4
5 cm

fig. 9

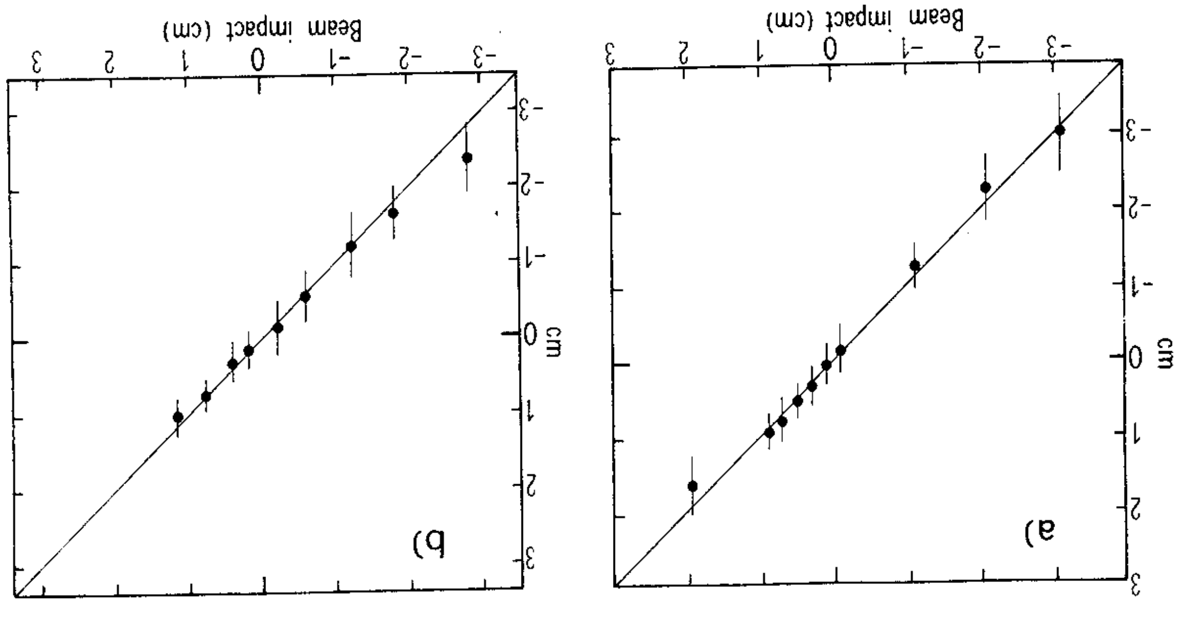
a)
b)
Beam impact (cm)
cm
-3
-2
-1
0
1
2
3

fig. 10

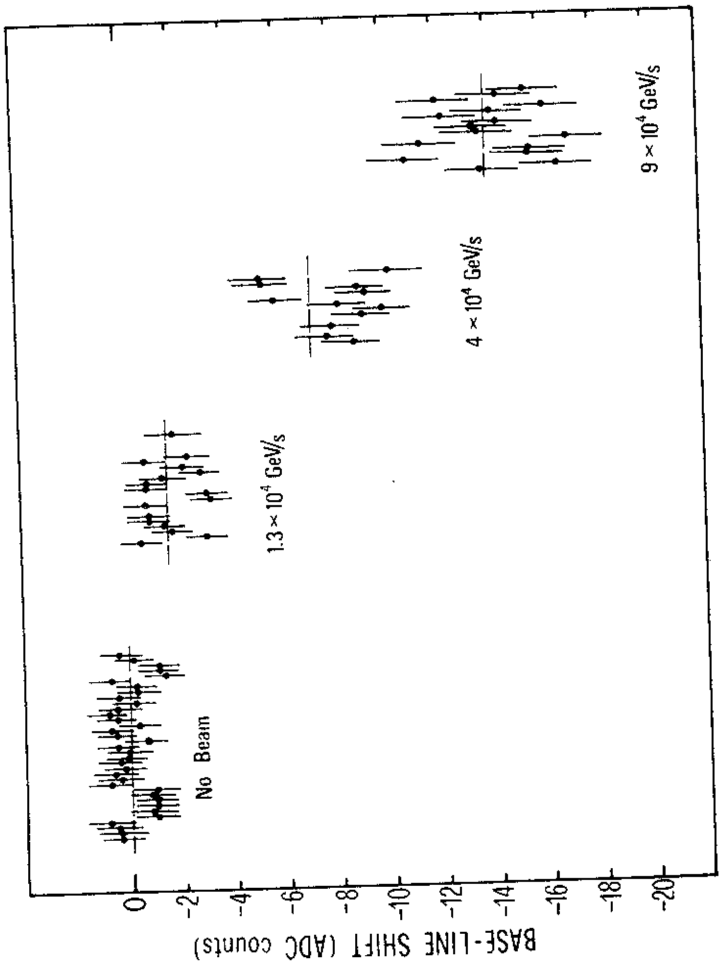
BASE-LINE SHIFT (ADC counts)
0
-2
-4
-6
-8
-10
-12
-14
-16
-18
-20
No Beam
1.3 × 10⁴ GeV/s
4 × 10⁴ GeV/s
9 × 10⁴ GeV/s

fig. 11